The American Journal of Pathology, Vol. 170, No. 5, May 2007

DOI: 10.2353/ajpath.2007.060772

Immunopathology and Infectious Disease

Emergence of Anti-Red Blood Cell Antibodies Triggers Red Cell Phagocytosis by Activated Macrophages in a Rabbit Model of Epstein-Barr Virus-Associated Hemophagocytic Syndrome

Wen-Chuan Hsieh,* Yao Chang,* Mei-Chi Hsu,* Bau-Shin Lan,† Guan-Chung Hsiao,† Huai-Chia Chuang,‡ and Ih-Jen Su*†

From the Division of Clinical Research, National Health Research Institutes, Tainan; and the Graduate Institutes of Microbiology‡ and Basic Medicine,‡ National Cheng Kung University College of Medicine, Tainan, Taiwan*

Hemophagocytic syndrome (HPS) is a fatal complication frequently associated with viral infections. In childhood HPS, Epstein-Barr virus (EBV) is the major causative agent, and red blood cells (RBCs) are predominantly phagocytosed by macrophages. To investigate the mechanism of RBC phagocytosis triggered by EBV infection, we adopted a rabbit model of EBV-associated HPS previously established by using Herpesvirus papio (HVP). The kinetics of virus-host interaction was studied. Using flow cytometry, we detected the emergence of antibody-coated RBCs, as well as anti-platelet antibodies, at peak virus load period at weeks 3 to 4 after HVP injection, and the titers increased thereafter. The presence of anti-RBCs preceded RBC phagocytosis in tissues and predicted the full-blown development of HPS. The anti-RBC antibodies showed cross-reactivity with Paul-Bunnell heterophile antibodies. Preabsorption of the HVP-infected serum with control RBCs removed the majority of anti-RBC activities and remarkably reduced RBC phagocytosis. The RBC phagocytosis was specifically mediated via an Fc fragment of antibodies in the presence of macrophage activation. Therefore, the emergence of anti-RBC antibodies and the presence of macrophage activation are both essential in the development of HPS. Our observations in this animal model provide a potential mechanism for hemophagocytosis in EBV infection. ***(Am J Pathol 2007, 170:1629–1639; DOI: 10.2353/ajpath.2007.060772)***

Hemophagocytic syndrome (HPS) is a fatal disorder frequently associated with microbial infections such as Epstein-Barr virus (EBV),[1] cytomegalovirus,[2] and recently, H5N1 influenza virus.[3] Although this syndrome is diverse in etiology and genetic association, HPS shares common clinical and laboratory features and is characterized by fever, hepatosplenomegaly, hypercytokinemia, cytopenia, coagulopathy, and a systemic proliferation of macrophages with phagocytosis of blood cells.[4–7] Among the viral pathogens responsible for HPS, EBV accounts for more than 60% of HPS cases in young children.[5,6] The pathogenesis of EBV-associated HPS has been proposed to result from a dysregulated cytotoxic T-cell response with macrophage activation in response to EBV infection in clinical conditions such as X-linked lymphoproliferative disorders and sporadic hemophagocytic lymphohistiocytosis (HLH).[7–10]

The phagocytic process by macrophages is by no means a random event but involves a meticulous interaction between ligands on the surface of phagocytosed cells and the receptors on the activated macrophages.[11,12] Because macrophage activation is a common phenomenon in infectious diseases, the relative rarity of HPS and the frequent association of HPS with EBV raise such a possibility that EBV may play a specific role in triggering HPS. Furthermore, the major blood cells engulfed by macrophages in EBV-associated HPS are red blood cells (RBCs) or platelets, distinct from the predominant lymphocytes in H5N1 influenza infection and other conditions such as Rosai-Dorfman disease.[3,13] To investigate why specific blood cells are selectively phagocytosed by macrophages in different conditions

Supported by the National Science Council and the National Health Research Institutes, Taiwan.

Accepted for publication January 25, 2007.

Address reprint requests to Dr. Ih-Jen Su, Division of Clinical Research, National Health Research Institutes, 367, Shen-Li Rd., Tainan, Taiwan. E-mail: suihjen@nhri.org.tw.

should help to clarify the pathogenesis of virus-associated HPS.

One clue to resolve this issue comes from the observations that virus infection may induce a wide spectrum of polyclonal B-cell and antibody responses against RBCs, platelets, lymphocytes, and endothelial cells.[14–16] The cell types that are opsonized, ie, prepared for phagocytosis by specific antibodies, may represent the selective targets of phagocytosis by activated macrophages mediated through Fc receptors. Of note, production of Paul-Bunnell (PB) heterophile antibodies that agglutinate RBCs is a prevailing serological marker for acute EBV infection or infectious mononucleosis.[15,17] The prevalence of anti-RBCs or heterophile antibodies in EBV infection may explain the frequent association of HPS with EBV. Therefore, we hypothesize that anti-RBC antibodies may play a pivotal role in triggering the phagocytosis of red cells in EBV-associated HPS. To test this hypothesis, we adopted a rabbit model of EBV-associated HPS previously established by Hayashi and colleagues[18–20] using EBV-related Herpesvirus papio (HVP). In this rabbit model, HVP is previously found to infect T and B cells, distinct from the predominant or exclusive infection of T or natural killer (NK) cells in HLH cases.[9,21] Although not entirely similar to the disease entity of human HLH, this animal model still represents a valuable tool to investigate the pathogenesis of virus-associated HPS. In this study, we extended the study to the kinetics of virus-host interaction, and the development of anti-virus and anti-RBC antibodies was longitudinally followed, with correlation to the presence of hemophagocytosis in tissues. *In vitro* and *ex vivo* phagocytosis assay was further performed to clarify the role of anti-RBC antibodies in RBC phagocytosis by activated macrophages mediated via Fc receptor.

Materials and Methods

Rabbit Model of EBV-Associated HPS

The rabbit model of EBV-associated HPS was previously established by Hayashi and colleagues[18] using the EBV homologue virus HVP. The HVP-producing baboon lymphoblastoid cell line 594S was cultured in RPMI 1640 medium (Life Technologies, Inc., Grand Island, NY) supplemented with 10% heat-inactivated fetal bovine serum (ICN, Aurora, OH) and 100 U/ml penicillin-streptomycin (Life Technologies, Inc.). Culture supernatants of 594S cells were centrifuged at 8000 $\times$ *g* for 30 minutes to remove cell debris, filtered with a 0.45-μm filter (Millipore, Billerica, MA), and then centrifuged at 100,000 $\times$ *g* (L-100XP; Beckman Coulter, Hialeah, FL) for 60 minutes to obtain concentrated virus stocks. New Zealand White rabbits (each weighing $\sim$2 kg) were obtained from Taiwan Livestock Research Institute (Tainan, Taiwan). Each rabbit was inoculated intravenously with virus stocks concentrated from 200 ml of culture supernatants of 594S cells [containing $\sim 5 \times 10^7$ copies of HVP as quantified by real-time polymerase chain reaction (PCR)]. Control rabbits were inoculated with phosphate-buffered saline (PBS).

Histopathological and Immunohistochemical Examinations

After inoculation with virus pellets, rabbits were sacrificed weekly under euthanasia with excess pentobarbital sodium (MTC Pharmaceuticals, Hamilton, ON, Canada). Control rabbits were sacrificed until all of the HVP-infected rabbits died of illness. The organs, including spleen, lymph nodes, livers, kidneys, thymus, lungs, and spinal cord, were examined macroscopically and then fixed with 3.7% formalin. The formalin-fixed, paraffin-embedded tissue blocks were sectioned at 3- to 5-μm thickness and stained for conventional histopathology with hematoxylin and eosin. Bone marrow and blood smears of rabbits were stained with a modified Wright or Liu A/Liu B stain.

For immunohistochemical studies of the distribution of T cells and B cells in tissues, freshly frozen specimens were sectioned at 5-μm thickness and immunostained with monoclonal mouse anti-human CD79α (B-cell marker, cross-reaction with rabbit CD79α) (DAKO, Glostrup, Denmark) and anti-CD5 (T cell) (Serotec Ltd., Oxford, UK) for 60 minutes at room temperature. The clone of CD5 monoclonal antibody used in this study is specific for T cells and does not cross-react with B cells. Cells were then washed twice with PBS and immunoreacted with goat anti-mouse horseradish peroxidase-conjugated IgG (horseradish peroxidase) (Amersham Bioscience, London, UK) for 60 minutes at room temperature. After washing, the sections were reacted with AEC (3-amino-9-ethylcarbazole) substrate (DAKO) and then examined under a microscope.

Detection of Antibody Responses to HVP Viral Capsid Antigen (VCA) in Rabbits

Anti-VCA IgG in sera was determined by an indirect immunofluorescence assay using EBV/indirect immunofluorescence assay slides (Meridian Bioscience, Cincinnati, OH). Different dilutions of rabbit sera (1:10 $\sim$ 1:640) were added to each well of EBV/indirect immunofluorescence assay slides and incubated for 30 minutes at room temperature. The slides were washed with PBS and then reacted with fluorescein isothiocyanate (FITC)-labeled goat anti-rabbit IgG (Jackson ImmunoResearch, West Grove, PA). After further incubation at room temperature for 30 minutes, slides were washed and observed under a fluorescence microscope. For controls, secondary antibody alone (FITC-labeled anti-rabbit IgG) and another irrelevant secondary antibody, FITC-labeled goat anti-mouse IgG (Jackson ImmunoResearch), were simultaneously run on the same test.

Immunomagnetic Purification of T Cells, B Cells, and Monocytes/Macrophages in Peripheral Blood Mononuclear Cells (PBMCs) and Spleen

Mononuclear cells of rabbits were isolated from whole blood and spleen by Ficoll gradient separation and la-

beled by incubating with mouse anti-rabbit IgM (B cells), anti-rabbit CD5 (T cells), or anti-human CD14 (cross-reaction with rabbit CD14) (Serotec Ltd.) for 15 minutes at room temperature. Cells were then washed twice with PBS and magnetically labeled with goat anti-mouse IgG MicroBeads (Miltenyi Biotec, Auburn, CA) for 15 minutes at 4°C. After washing, the $CD5^+$ T cells, IgM^+ B cells, or $CD14^+$ monocytes/macrophages were separated by an immunomagnetic procedure incorporating the MACS system (Miltenyi Biotec).

PCR Detection of HVP DNA in PBMCs or Component Fractions of T Cells, B Cells, and Monocytes/Macrophages

DNA extraction was performed according to the manufacturer's description of QIAamp DNA blood kit (Qiagen GmbH, Hilden, Germany). For detection of HVP virus genome, we used one primer pair for HVP EBNA1 (HPNA-1S: 5′-CTGGGTTGTTGCGTTCCATG-3′, HPNA-1A: 5′-TTGGGGGCGTCTCCTAACAA-3′) and two primer pairs for HVP EBNA2 (HPNA2-231S: 5′-ACCACTGGGA-CCAGTTTGGT-3′, HPNA2-1612A: 5′-AGAGGACTGAG-GTTCTTGC-3′; PNA2-1485S: 5′-AGCCTAGGCCCAATA-GCTCA-3′ and HPNA2-1691A: 5′-CCTCCCATTGGTTG-TCAGGG-3′) as previously described.[18] β-Actin primers were used as an internal control: AC3: 5′-GGAGCCTTG-AATACACCCAA-3′ and AC4: 5′-GAGGCGTACAGGGA-TAGCA C-3′. For each PCR reaction, 35 cycles were performed on 50 ng of DNA in 25 μl of PCR reaction mixture, which consisted of 50 nmol/L KCl, 10 mmol/L Tris-HCl, pH 8.3, 1.5 mmol/L $MgCl_2$, 200 nmol/L dNTP, 0.2 μmol/L primers, and 1.25 U of *Taq* polymerase (Takara, Shiga, Japan).

Quantification of HVP Virus Load by Real-Time PCR

For detection of HVP virus load in sera of infected rabbits, quantitative real-time PCR was performed using the LightCycler 1.5 (Roche Diagnostics GmbH, Mannheim, Germany) and LightCycler-FastStart DNA Master SYBR Green I (Roche Diagnostics GmbH). Virus DNA in rabbit sera were extracted by QIAamp DNA mini kit (Qiagen GmbH) according to the manufacturer's protocol. A total of 4 μl of sample DNA was used in a reaction volume of 20 μl, and the assay contained 4 mmol/L magnesium chloride, 0.25 μmol/L of each primer, 2 μl of 1× LightCycler FastStart DNA Master SYBR Green I mixture. The reaction conditions for the assay were as follows: one segment of denaturation at 95°C for 10 minutes; 45 cycles of amplification at three segments of 95°C for 10 seconds, 57°C for 5 seconds, and 72°C for 10 seconds; three segments of melting at 95°C, 65°C for 15 minutes, and 95°C; and finally one segment of cooling at 40°C for 30 seconds. The primers used in this assay were HPNA2-1485S and HPNA2-1691A.

In Situ *Hybridization to Detect Virus-Encoded Small RNA, EBER1*

Rabbit spleens, lymph nodes, thymuses, lungs, and livers were fixed with formalin and paraffin-embedded. Sections of 3-μm thickness were put onto glass slides and subjected to detection of EBER1. *In situ* hybridization was performed according to the manufacturer's protocol provided in the EBV probe in situ hybridization kit (Novocastra Laboratories Ltd., Newcastle on Tyne, UK).

Flow Cytometric Detection of Antibody-Coated Red Cells and Anti-Platelets in HVP-Infected Rabbits

Rabbit blood samples were collected before and after the inoculation with HVP. Rabbit red cells were isolated from whole blood by Ficoll gradient separation, washed twice with PBS, and then incubated with FITC-labeled anti-rabbit immunoglobulin (DAKO) for 30 minutes. After setting forward scatter/side scatter detectors to log mode and gating the RBC region, surface fluorescence on the rabbit red cells was measured by FACSCalibur (Becton, Dickinson and Company, Franklin Lakes, NJ) and analyzed by CellQuest software. FITC-labeled mouse IgG (Becton, Dickinson and Company) was used as isotype control in this experiment.

To clarify whether anti-platelet antibodies were also present in this animal model, assays for anti-platelet antibodies were also performed. Platelet-rich plasma was separated from whole blood by centrifugation (250 × *g* for 10 minutes). After washing and counting, 10^6 platelets were incubated with HVP-infected rabbit serum for 30 minutes. Platelets were then washed twice with PBS and double-labeled with anti-rabbit CD41/CD61 PE (Serotec Ltd.) and anti-rabbit Ig FITC (DAKO) for another 30 minutes. After washing with PBS, fluorescence on platelets was measured and analyzed by FACSCalibur. For cellular enzyme-linked immunosorbent assay, 10^7 platelets were seeded in each well of a 96-well plate and then incubated at 37°C for 2 hours. For fixation, 4% paraformaldehyde was added into each well after carefully washing each well and then incubated at room temperature for 15 minutes. After blocking with PBS/1% bovine serum albumin, different dilutions of rabbit plasma were added into wells and incubated at room temperature for 2 hours. Horseradish peroxidase-conjugated anti-rabbit immunoglobulin (Amersham Biosciences) was then added after washing the plate and incubated for 1 hour. Finally, tetramethyl benzidine substrate was applied to elicit a chromogenic signal, and the plate was measured under an enzyme-linked immunosorbent assay reader.

Detection of PB Heterophile Antibodies and Preabsorption Test

Determination of PB heterophile antibodies in rabbit sera was performed with Monospot latex kit (Meridian Bioscience), which contains the PB heterophile determi-

nants. Briefly, 50 μl of sample was added on one well of the disposable slide, and then a drop of latex reagent was added next to the drop of sample. After mixing and rotating gently for 3 minutes, the mixture was examined for the presence or absence of agglutination. To investigate whether heterophile antibodies represent the predominant component of anti-red cell antibodies in the infected serum, a preabsorption test was performed. The infected rabbit sera were preincubated with 1×10^8 normal rabbit red cells for 30 minutes at 37°C twice before performing the agglutination assay.

In Vitro *Phagocytosis Assay*

The promonocytic cell line U937 was differentiated by activation with 5 ng/ml phorbol ester (TPA) (Sigma, St. Louis, MO) for 48 hours. FITC-labeled latex beads (Sigma) were added into TPA-treated or untreated U937 cells and incubated for 2 hours at 37°C. After washing four times with PBS, phagocytosis could be observed under fluorescence microscopy. For investigating phagocytosis of red cells by macrophages, normal human red cells and Coombs-treated cells (Gamma Biologicals Inc., Houston, TX) were labeled with FITC using the Flurorotag FITC conjugation kit (Sigma). FITC-labeled normal human red cells and FITC-labeled Coombs-treated cells were used in this study. The FITC-labeled target cells were incubated with TPA-activated U937 cells at 37°C for 2 hours. After incubation, unengulfed red cells were lysed by RBC lysis buffer, and the remaining cells were examined by fluorescence microscopy or flow cytometry.

Antibody Coating and ex Vivo *Phagocytosis of Rabbit Red Cells*

Rabbit monocytes were isolated from PBMCs by using the immunomagnetic approach mentioned above. The rabbit monocytes were activated by TPA and tested for the engulfment of FITC-labeled normal rabbit red cells that were precoated or not coated with HVP-infected rabbit sera. After co-incubation of activated monocytes and red cells for 2 hours, phagocytosis of red cells was examined by fluorescence microscopy.

Purification of Fab and Fc Fragments for Phagocytosis Assay

To determine whether phagocytosis of red cells is mediated via Fc fragments, Fab and Fc fragments were separately prepared by papain digestion using the Immuno-Pure Fab preparation kit (Pierce, Rockford, IL). In brief, 10 mg of purified human IgG (Sigma) was digested with immobilized papain for 5 hours at 37°C. Then chromatography was used to purify Fab and Fc fragments of IgG on a column with protein G (Pierce). The Fc, Fab fragments, or whole IgG were added as blockers (at a final concentration of 1 mg/ml) in the phagocytosis assay described above.

Results

Gross Observations and Histopathological and Immunohistochemical Studies of HPS in the Rabbit Model

A total of 11 rabbits were used for this study, eight receiving HVP inoculation and three as control. Five HVP-infected rabbits were serially sacrificed under euthanasia to observe the dynamic virus-host interaction and the sequential development of diseases. The remaining three HVP-infected rabbits developed fulminating HPS and died within 1 month (on days 23 to 30 after virus inoculation). They appeared physically healthy until the last week before they died. The rabbits first lost appetite and then became emaciated. A few of them had rhinorrhea admixed with blood and then developed dyspnea. All three control rabbits were free from symptoms and remained healthy at the end of the experiment.

Necropsy of the infected rabbits revealed dark purple (congestion) and swollen lymph nodes, as well as hepatosplenomegaly. The kidneys and thymuses looked normal, but lungs showed congestion and edema. All control rabbits looked otherwise normal. Histopathological examinations of the infected rabbit tissues showed progressive lymphoid depletion in spleen and lymph nodes (Figure 1A) with lymphoid infiltration of predominantly $CD5^+$ T cells around perivascular areas in many organs such as livers, kidneys, and lungs. The liver showed mild fatty changes with portal infiltration of predominant $CD5^+$ T-lymphoid cells. The bone marrow showed mild hyperplasia at day 20 but progressed to marked hypoplasia at death. The histological pictures of hemophagocytosis first appeared at 3 weeks after HVP inoculation, with predominant engulfment of red cells by macrophages in the sinuses of spleens, lymph nodes, and bone marrow of HVP-infected rabbits (Figure 1B). The severity of red cell engulfment by activated macrophages was associated with disease progression. Plasma cells, atypical lymphocytes, and nucleated red cells could also be observed in blood smears of HVP-infected rabbits with HPS (data not shown).

Detection of Antibodies to VCA and Viral Genomes in PBMCs and Tissues of HVP-Inoculated Rabbits

All sera obtained from HVP-inoculated rabbits were anti-VCA IgG-positive, whereas sera from the preinoculated rabbits and from control rabbits showed negative reactivity. Although seroconversion varied in titers among the HVP-infected rabbits, antibodies to VCA became detectable on day 19 and persisted thereafter (Figure 2A).

The presence of viral genomes in PBMCs from infected rabbits was assessed by PCR to detect EBNA1 and EBNA2 gene regions of HVP DNA. As shown in Figure 2B (top), HVP-EBNA2 genomes (the same for EBNA1, data not shown) were detectable in PBMCs from day 19 after virus inoculation. Quantitative PCR studies showed that HVP DNA in rabbit sera was de-

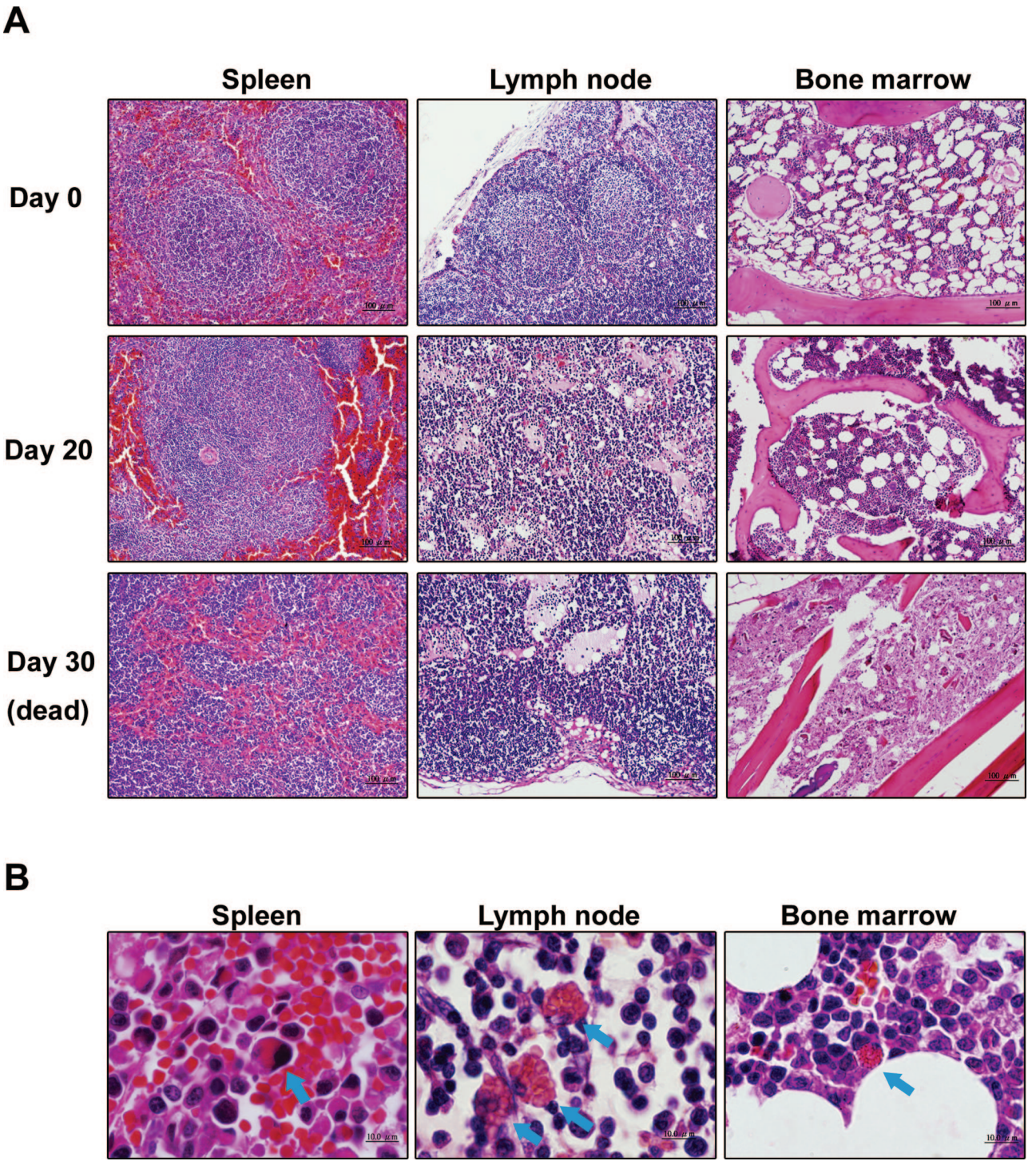

Figure 1. Histopathological features of HVP-infected rabbits. **A:** The histopathological features of spleens, lymph nodes, and bone marrow (BM) on days 0, 20, and 30 after virus inoculation. The pictures on day 30 represent necropsy findings and revealed general lymphoid depletion and BM hypoplasia. **B** exemplifies the high-power magnification of the findings on day 22 to reveal hemophagocytosis (marked with **blue arrows**) in spleens, lymph nodes, and bone marrow. All of the sections were stained with H&E. Original magnifications: ×20 (**A**); ×100 (**B**).

tectable from day 12, and the viral load peaked during weeks 3 to 4 after HVP inoculation and declined thereafter. HVP DNA could also be detected by PCR in most other tissues, such as spleens, lymph nodes, livers, and lungs from HVP-infected rabbits (data not shown). By immunomagnetic purification, HVP DNA could be detected in the fractions of purified $CD5^+$ T cells, IgM^+ B cells, and $CD14^+$ monocytes of PBMCs in HVP-infected rabbits from day 19 after virus inoculation (Figure 2B, bottom). *In situ* EBER1 hybridization was further performed on formalin-fixed tissues of HVP-infected rabbits. EBER1 RNA of HVP was detectable in

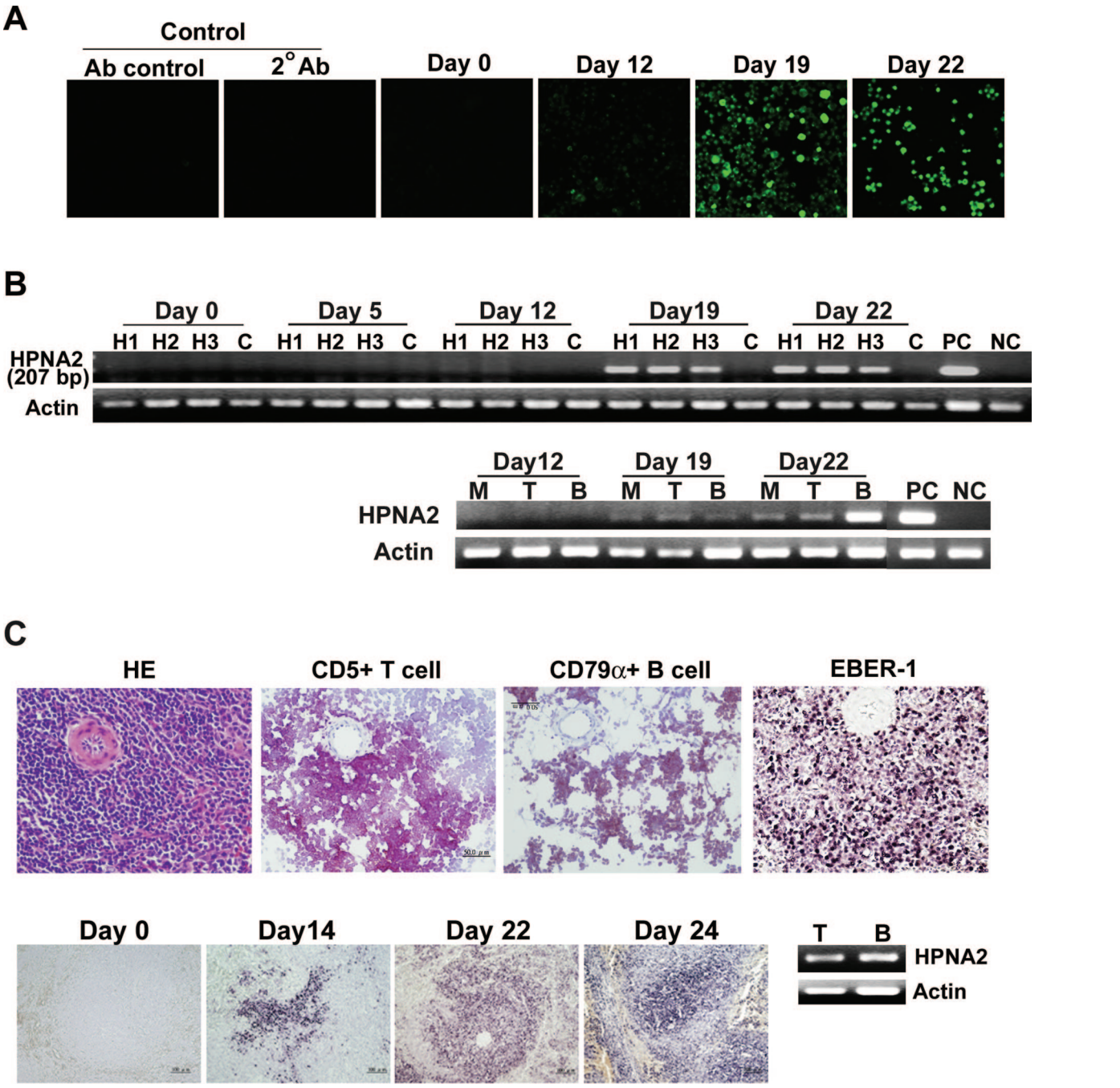

Figure 2. Kinetics of antibody response against VCA and detection of HVP virus DNA and RNA. **A:** Anti-VCA antibodies in rabbit sera, as demonstrated by indirect immunofluorescence assay using commercial slides. Anti-VCA antibodies became detectable on day 19 after HVP inoculation. Control studies included different species antibody control (Ab control, anti-mouse IgG FITC) and secondary antibody control (two Abs, goat anti-rabbit IgG FITC). **B** (top)**:** Detection of HVP-EBNA2 gene (207 bp) in rabbit PBMCs at different time points after virus inoculation. H1, H2, and H3: PBMCs from three rabbits inoculated with HVP. **C:** Uninfected control rabbit. PC: 594S cells (HVP-producing cells as positive control); NC: U937 cells as negative control. By immunomagnetic purification of $CD5^+$ T cells, IgM^+ B cells, and $CD14^+$ monocytes, HVP-EBNA2 could be detected in the fractions of purified T cells (T), B cells (B), and monocytes (M) of PBMCs (**B**, bottom) in HVP-infected rabbits since day 19 after virus inoculation. **C** (top)**:** Specific lymphoid maker (CD79α and CD5) staining as well as EBER1 *in situ* hybridization on spleen cells on day 22 after HVP inoculation. **C** (bottom)**:** HVP EBER1 *in situ* hybridization on different time points after HVP inoculation. The EBER1-positive signals appeared first in the marginal zones of white pulp of spleen and increased in numbers thereafter. HVP DNA could be detected in both T and B cells obtained from splenocytes collected on day 22 after HVP inoculation (**C**, bottom right). By real-time PCR analysis, the mean of virus load in B cells was 414 copies per 100 ng of cell DNA, higher than the 225 copies in T cells. Original magnifications: ×200 [**A**, **C** (top)]; ×100 (**C**, bottom).

lymphocytes of spleens (Figure 2C, top), lymph nodes, and thymuses. The EBER1 signals were first detected at the marginal zone of white pulp of spleens on day 14 and then extensively in spleens (Figure 2C, bottom) and lymph nodes in the following weeks. EBER1 could also be detected in most infiltrating lymphocytes of lungs and livers obtained in week 4 after HVP inoculation or at necropsy. Immunohistochemical studies revealed that the infiltrating lymphoid cells in liver and lungs were mostly CD5 T cells, and only rarely B cells

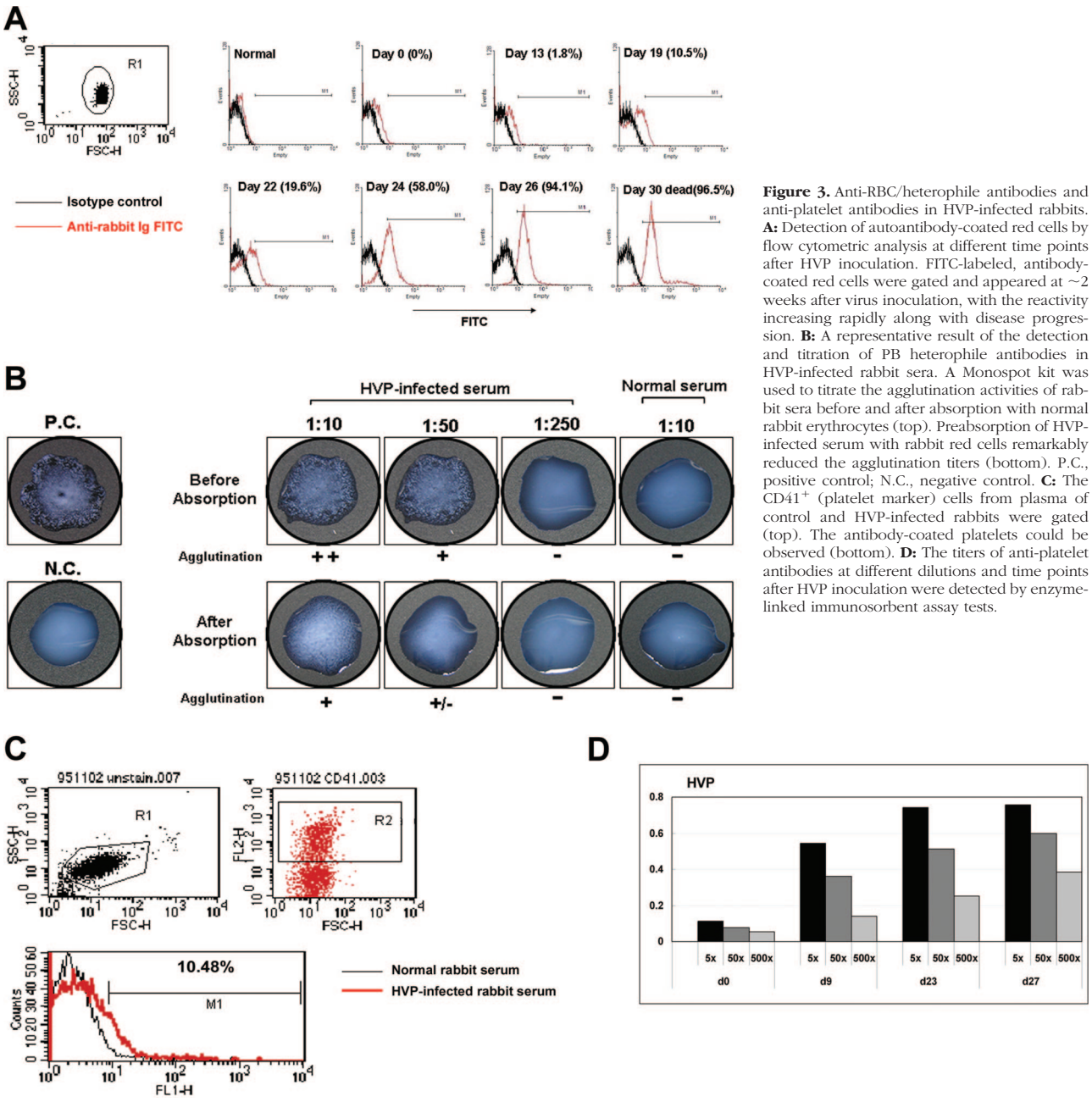

Figure 3. Anti-RBC/heterophile antibodies and anti-platelet antibodies in HVP-infected rabbits. **A:** Detection of autoantibody-coated red cells by flow cytometric analysis at different time points after HVP inoculation. FITC-labeled, antibody-coated red cells were gated and appeared at ~2 weeks after virus inoculation, with the reactivity increasing rapidly along with disease progression. **B:** A representative result of the detection and titration of PB heterophile antibodies in HVP-infected rabbit sera. A Monospot kit was used to titrate the agglutination activities of rabbit sera before and after absorption with normal rabbit erythrocytes (top). Preabsorption of HVP-infected serum with rabbit red cells remarkably reduced the agglutination titers (bottom). P.C., positive control; N.C., negative control. **C:** The $CD41^+$ (platelet marker) cells from plasma of control and HVP-infected rabbits were gated (top). The antibody-coated platelets could be observed (bottom). **D:** The titers of anti-platelet antibodies at different dilutions and time points after HVP inoculation were detected by enzyme-linked immunosorbent assay tests.

(data not shown). The *in situ* EBER1 signals correlated to the white pulps of the spleen, which contained B- and T-immunoreactive cells (Figure 2C, top). To confirm the specificity of HVP-infected cells, immunomagnetic purification and fractionation of T and B cells was performed on spleen lymphocytes. HVP DNA could be detected in the fractions of T and B cells in spleen (Figure 2C, bottom right). Quantitative real-time PCR analysis revealed that B cells contained a mean of 414 copies of HVP genome per 100 ng of cell DNA, higher than the 225 copies of HVP genome in T-cell fraction. The $CD14^+$ fraction contained too few cells to be available for DNA extraction and further analysis.

Detection of Anti-RBC Antibodies, PB Heterophile Antibodies, and Anti-Platelet Antibodies in Serum of HVP-Infected Rabbits

Using FITC-labeled anti-rabbit immunoglobulin in flow cytometric analysis, we found that red cells from HVP-infected rabbits were coated with antibodies. The antibody-coated red cells appeared at around 2 weeks after virus inoculation, and the reactivities increased rapidly thereafter: 2% on day 13, 20% on day 22, and 60% on day 24. In the last week immediately before death, more than 90% of red cells were coated with antibodies (Figure 3A).

Table 1. Titers of Anti-RBC and Heterophile Antibodies at Different Time Points (Day 0 to Day 26) after HVP Infection in Three Rabbits

	H1		H2		H3		Control	
	Anti-RBC (%)	Heterophile antibody	Anti-RBC (%)	Heterophile antibody	Anti-RBC (%)	Heterophile antibody	Anti-RBC (%)	Heterophile antibody
d0	<5		<5		<5		<5	
d5	<5		<5		<5		<5	
d12	5.4	1:10~1:50	5.6	+/−	<5		<5	
d19	30.9	1:50	5.4	1:10	6.6	+/−	<5	
d22	76.9	1:50~1:250	19.3	1:50~1:250	18.1	1:10~1:50	<5	
d26	94.1	1:50~1:250	89.1	1:250	95.4	1:50	<5	

d, day.

Considering that patients with infectious mononucleosis produce heterophile antibodies that agglutinate red cells, we speculated that a link may exist between the heterophile antibodies and anti-red cell autoantibodies in our rabbit model. An agglutination test using a Monospot kit showed that all HVP-infected rabbits produced PB heterophile antibodies, whereas control rabbits did not (Figure 3B, top). The antibody-coated red cells closely correlated to the titers of heterophile antibodies during disease progression (Table 1). Preabsorption of HVP-infected sera with normal rabbit erythrocytes could significantly reduce the agglutination activity of heterophile antibodies. The titers of heterophile antibodies decreased from 1:250 to below 1:50 after preabsorption (Figure 3B, bottom). These results indicate that the anti-red cell antibodies in the serum of HVP-infected rabbits cross-reacted with PB heterophile antibodies in this rabbit model.

In this rabbit model, we observed that the platelets in HVP-infected rabbits decreased with disease progression (data not shown). To clarify whether the HVP-infected rabbits also developed anti-platelet antibodies, we gated $CD41^+$ (platelet marker, Figure 3C) cells to observe the antibody-coated platelets. As shown in Figure 3D, the antibody-coated platelets could be observed at day 9 after HVP inoculation and, similar to anti-RBC antibodies, the titers of anti-platelet antibodies increased with correlation to the severity of diseases.

Figure 4, A and B, summarizes the kinetics of virus-host interaction in this HPS animal model. The first event detectable after virus inoculation was the appearance of HVP DNA in rabbit sera at day 12, followed by the production of anti-VCA antibodies in sera and the presence of viral genomes in PBMCs and tissues at day 19. The production of anti-RBC/heterophile antibodies developed at a relatively late stage, usually occurring when the virus load peaked during weeks 3 to 4 after HVP inoculation, and increased rapidly thereafter. Notably, the red cell phagocytosis in rabbit tissues could only be observed after the emergence of anti-RBC antibodies, suggesting that the coating of red cells with antibodies is a prerequisite for phagocytosis of red cells. The increasing titers of anti-RBC antibodies represented a reliable indicator to predict the full-blown diseases and impending mortality in HVP-infected rabbits.

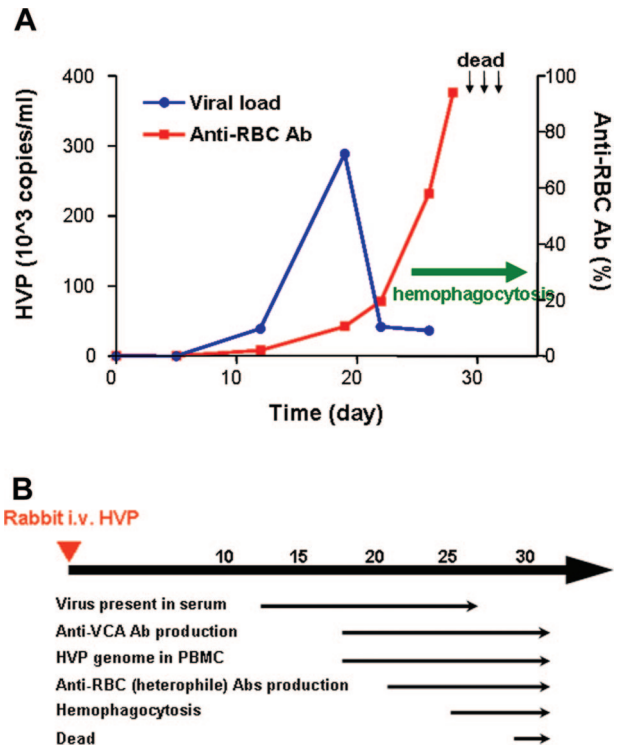

Figure 4. Kinetics of virus-host interaction during the development of HPS. **A:** The kinetics of viral loads in sera and the titers of autoantibody-coated red cells after HVP inoculation, with correlation to the presence of hemophagocytosis in tissues. The time points of death in three rabbits were indicated by **arrows**. **B** summarizes the time table of several clinical and laboratory parameters after HVP infection of rabbits.

Contribution of Anti-RBC/Heterophile Antibodies to Red Cell Phagocytosis by Activated Macrophages

To clarify whether both the presence of antibodies against red cells and macrophage activation are essential for the hemophagocytic process, we performed serial *in vitro* phagocytic studies. First, the human promonocytic cell line U937 was treated with or without TPA and tested for the activity to engulf FITC-labeled latex beads. U937 cells could phagocytose the fluorescent beads only when the U937 cells were preactivated by TPA (data not shown). Furthermore, the TPA-treated U937 cells could only engulf Coombs-treated cells (Figure 5A, right; Coombs cell) but not control red cells (Figure 5A, control), indicating that the coating of

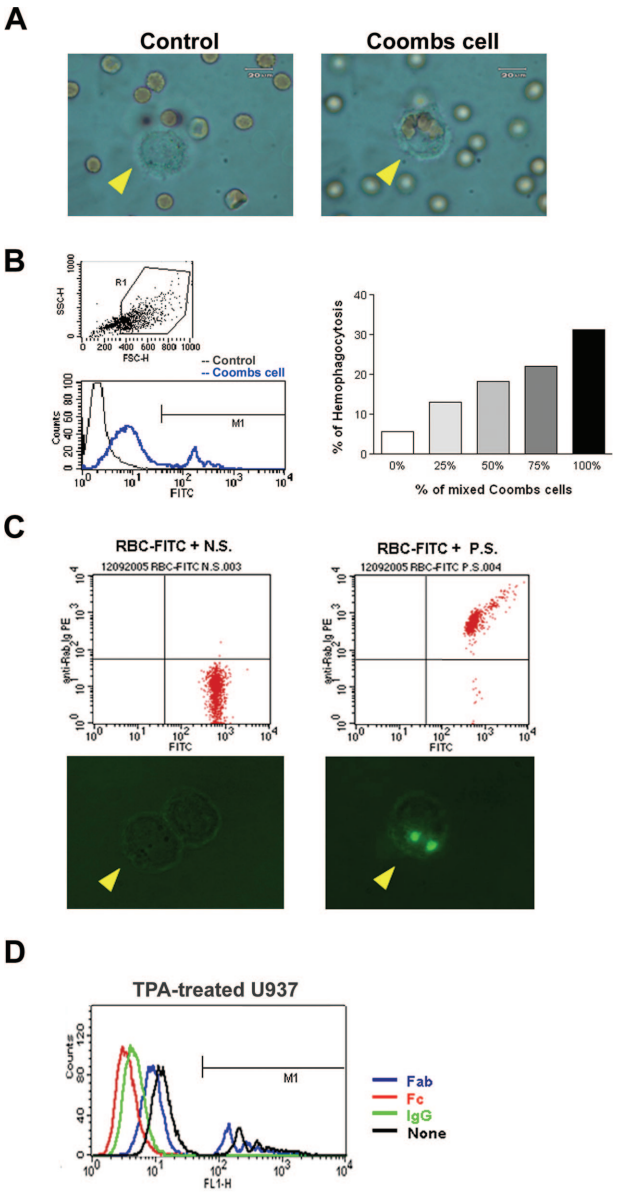

Figure 5. Anti-red cell/heterophile antibody-mediated phagocytosis assay *in vitro* and *ex vivo*. **A:** *In vitro* study to show the specific engulfment of Coombs cells, but not the control RBCs, by activated macrophages (**arrowhead**). **B:** *In vitro* study to show the dose-dependent manner of phagocytosis of Coombs cells by activated macrophages. TPA-activated U937 cells were gated (top left). The FITC intensities were gated at M1 region (bottom left). The activities of RBC phagocytosis by macrophages increased with the ratio of Coombs cells (right). **C:** *Ex vivo* assay of phagocytosis of antibody-coated rabbit red cells by TPA-activated rabbit monocytes. Top panel shows flow cytometric analysis of FITC-labeled RBCs treated with either control serum (N.S.) or HVP-infected serum (P.S.) (top). The activated macrophages engulfed only the red cells incubated with HVP-infected serum (bottom right), but not with control serum (bottom left). **D:** IgG molecules and Fc fragments, but not Fab fragments, completely inhibited antibody-mediated phagocytosis of Coombs cells by TPA-treated U937 cells. The FITC intensities over the M1-defined region mark the measured fluorescence intensity fraction of Coombs cell phagocytosis.

a red cell with anti-RBC antibodies was required for phagocytosis by activated macrophages. For clarification of the relationship between the titers of antibodies present on red cell surfaces and the degree of RBC phagocytosis, different ratios of antibody-coated RBCs were used to measure the percentages of phagocytosis by flow cytometry. The fraction of macrophages was gated (Figure 5B, top left), and the fluorescence intensity of the gated macrophages was measured. The Coombs cell study showed a higher nonspecific background attributable to the adherence of RBC lysate to the surface of activated macrophages. The fluorescence intensity of phagocytosed Coombs cells was measured over the M1-defined region (Figure 5B, bottom left). As shown in Figure 5B (right), the activities of RBC phagocytosis by macrophages increased with the ratio of Coombs cells (human IgG-coated RBCs). *Ex vivo* phagocytosis assay further showed that the TPA-activated rabbit monocytes could engulf rabbit erythrocytes only when pretreated with HVP-infected rabbit sera (Figure 5C, right), but not the uninfected sera (Figure 5C, left). To define clearly the specificity of the immunoglobulin fragments that reacted with macrophages, excess Fab fragments, Fc fragments, or the whole IgG molecules were used to compete with the antibodies of Coombs cells. Figure 5D demonstrates that Fc fragments as well as whole IgG molecules, but not Fab fragments, could completely block the engulfment of Coombs-treated cells by TPA-activated U937 cells, indicating that phagocytosis is mediated through Fc receptor. Taken together, the data shown above indicate that both the presence of anti-red cell antibodies and macrophage activation are essential for RBC phagocytosis, which is mediated via Fc fragments.

Discussion

For decades, physicians and investigators have been puzzled over the mechanism of hemophagocytosis in human diseases. In this study, we demonstrated by *in vivo*, *ex vivo*, and *in vitro* studies that the emergence of anti-RBC, and probably anti-platelet antibodies, after HVP infection is pivotal to trigger the phagocytic process in this rabbit model of EBV-associated HPS. Based on the dynamic kinetics of virus-host interaction *in vivo* as shown in Figure 4, the emergence of anti-RBC antibodies always preceded the development of RBC phagocytosis in tissues and the increasing titers of anti-RBC antibodies predicted the full-blown development of HPS and the impending mortality of HVP-infected rabbits. Given that this rabbit model of EBV-associated HPS is not entirely similar to human HLH cases, the findings we observed in this study can still provide valuable information on the mechanism of hemophagocytosis in virus-associated HPS.

Although the presence of anti-RBC antibodies or PB heterophile antibodies in this animal model can explain the frequent association of childhood HPS with EBV, the ubiquitous EBV infection and the relative rarity of EBV-associated HPS, however, challenge the role of anti-RBC antibodies in the development of EBV-HPS. As shown in this study, we demonstrated that both the phagocytic process and the specific types of blood cells phagocytosed by macrophages represent nonrandom biological events. In the absence of anti-RBC antibodies, red cell phagocytosis did not occur even in the presence of ac-

tivated macrophages and vice versa. This observation may therefore explain the relative infrequency of HPS in most viral infections other than those observed with EBV and in virus-associated HLH patients.

EBV-associated HPS usually develops in patients with abnormal immune disorders such as X-linked lymphoproliferative disorders[22] or in rare conditions in which EBV infects T or NK cells such as HLH and NK/T cell lymphoma.[9,10,23] In X-linked lymphoproliferative disorders, the mutation of a suppressor SAP protein leads to dysregulated CTL response in primary EBV infection.[24,25] In sporadic HLH patients, EBV usually infects T or NK cells rather than B cells, and EBV latent membrane protein-1 has been demonstrated to initiate the TRAFs/NF-κB/SAP/ERK signaling pathway to activate T cells and up-regulate Th1 cytokine secretion.[25–28] Alternatively, HLH may result from mutations of perforin genes, leading to an ineffective CTL response to EBV infection.[21] Distinct from the predominant or exclusive infection of T or NK cells by EBV in HLH,[9,21] HVP infects T cells, B cells, and possibly macrophages in this rabbit model. Virus infection of B cells may induce polyclonal activation of B lymphocytes and leads to the formation of a wide variety of autoantibodies, including those directed against smooth muscle, blood groups, lymphocytes, platelets, and erythrocytes.[29–31] Summarizing the data, we presented in this study, we propose that the development of HPS requires two essential events, one involving dysregulated CTL immune response, which results in hypersecretion of Th1 cytokines and the subsequent activation of macrophages, and the other branch involving the autoreactive polyclonal B-cell response that produces autoantibodies against blood cells. Whether monocytes/macrophages can be infected by EBV is still controversial. Recent studies, however, have demonstrated the capability of EBV to infect and replicate in freshly isolated human monocytes.[32] The infection of macrophages by EBV may further activate macrophages. In this animal model, the infectivity of tissue macrophages by HVP was inconclusive because of too few cells to be obtained for flow cytometric analysis. However, HVP DNA could be detected in the $CD14^+$ monocyte fraction in PBMC. Therefore, the possibility of HVP infection of macrophages may exist. The infection of monocytes/macrophages by EBV/HVP may further activate the macrophages to secrete monokines and make the cytokine storm worse in HPS.

Among the wide variety of autoantibodies produced, PB heterophile antibodies are specifically associated with primary EBV infection.[17] In past decades, extensive efforts have been given to study cross-species reactivity patterns and antigenic epitopes of PB heterophile antibodies.[17,33] Epitopes of PB antibodies in erythrocyte membrane have been recognized to be sialoglycopeptides containing the *O*-linked disialyl Gal-GalNAc oligopeptide. This epitope forms the basis for commercially available kits currently used for antibody detection in the diagnosis of infectious mononucleosis and was adopted in this study. Several explanations have been proposed to describe the mechanism of developing heterophile antibodies in EBV infection. Molecular mimicry of host cell DNA or proteins to viral gene products is the most prevailing theory.[31,34] By preabsorption of HVP-infected sera with rabbit red cells in this study, the titers of heterophile antibodies were reduced significantly, suggesting that the PB heterophile antibodies may cross-react with or even represent the major components of anti-RBC antibodies in HVP-infected rabbit serum. One critical question is whether the finding of anti-RBC antibodies in this animal model can be applied to human HPS or HLH patients. We retrospectively retrieved serum samples from a total of 20 EBV-associated HPS patients for indirect Coombs test, and eight of them were positive (W.-C.H. and I.-J.S, unpublished data), suggesting that anti-RBC antibodies do exist in some of the EBV-HPS patients. We are now performing a prospective multicenter study using direct Coombs test to clarify the positivity of anti-RBC antibodies in EBV-HPS patients.

In this study, we further clarified the kinetics of virus-host interaction in this animal model of EBV-associated HPS.[18–20] The HVP viruses appear to first infect lymphoid cells in the marginal zone of spleens, followed by an extensive infection in spleen, lymph nodes, livers, and lungs before mortality. The rabbits developed symptoms and signs typical to that of human HPS such as coagulopathy, cytopenia, and depletion of lymphoid systems and bone marrow. Because of the limitation and commercial availability of antibodies against rabbits, especially those of cytokines and antigens of blood cells, a detailed description of cytokine changes is not available in this study. Although this HVP rabbit model of HPS is not entirely similar to human HLH cases, the findings we observed in this study can still provide valuable information to understand the pathogenesis of human EBV-HPS. Importantly, this animal model should also provide a valuable tool for designing the therapeutic trial to improve the management of virus-associated HPS patients.

References

1. Reisman RP, Greco MA: Virus-associated hemophagocytic syndrome due to Epstein-Barr virus. Hum Pathol 1984, 15:290–293
2. Aouad A, Dan ME, Alangaden GJ: Photo quiz. I. Reactive hemophagocytic syndrome caused by CMV infection. Clin Infect Dis 1998, 26:1295, 1439
3. To KF, Chan PK, Chan KF, Lee WK, Lam WY, Wong KF, Tang NL, Tsang DN, Sung RY, Buckley TA, Tam JS, Cheng AF: Pathology of fatal human infection associated with avian influenza A H5N1 virus. J Med Virol 2001, 63:242–246
4. Ost A, Nilsson-Ardnor S, Henter JI: Autopsy findings in 27 children with haemophagocytic lymphohistiocytosis. Histopathology 1998, 32:310–316
5. Su IJ, Hsieh HJ, Lee CY: Histiocytic medullary reticulosis: a lethal form of primary EBV infection in young children in Taiwan. Lancet 1989, 1:389
6. Chen RL, Su IJ, Lin KH, Lee SH, Lin DT, Chuu WM, Lin KS, Huang LM, Lee CY: Fulminant childhood hemophagocytic syndrome mimicking histiocytic medullary reticulosis. An atypical form of Epstein-Barr virus infection. Am J Clin Pathol 1991, 96:171–176
7. Janka GE: Familial hemophagocytic lymphohistiocytosis. Eur J Pediatr 1983, 140:221–230
8. Sumegi J, Huang D, Lanyi A, Davis JD, Seemayer TA, Maeda A, Klein G, Seri M, Wakiguchi H, Purtilo DT, Gross TG: Correlation of mutations of the SH2D1A gene and Epstein-Barr virus infection with clinical phenotype and outcome in X-linked lymphoproliferative disease. Blood 2000, 96:3118–3125
9. Su IJ, Chen RL, Lin DT, Lin KS, Chen CC: Epstein-Barr virus (EBV)

infects T lymphocytes in childhood EBV-associated hemophagocytic syndrome in Taiwan. Am J Pathol 1994, 144:1219–1225
10. Su IJ, Wang CH, Cheng AL, Chen RL: Hemophagocytic syndrome in Epstein-Barr virus-associated T-lymphoproliferative disorders: disease spectrum, pathogenesis, and management. Leuk Lymphoma 1995, 19:401–406
11. Aderem A, Underhill DM: Mechanisms of phagocytosis in macrophages. Annu Rev Immunol 1999, 17:593–623
12. Larroche C, Mouthon L: Pathogenesis of hemophagocytic syndrome (HPS). Autoimmun Rev 2004, 3:69–75
13. Kara IO, Ergin M, Sahin B, Inal S, Tasova Y: Sinus histiocytosis with massive lymphadenopathy (Rosai-Dorfman's disease) previously misdiagnosed as Toxoplasma lymphadenitis. Leuk Lymphoma 2004, 45:1037–1041
14. Papesch M, Watkins R: Epstein-Barr virus infectious mononucleosis. Clin Otolaryngol Allied Sci 2001, 26:3–8
15. Haukenes G, Viggen B, Boye B, Kalvenes MB, Flo R, Kalland KH: Viral antibodies in infectious mononucleosis. FEMS Immunol Med Microbiol 1994, 8:219–224
16. Lin YS, Lin CF, Fang YT, Kuo YM, Liao PC, Yeh TM, Hwa KY, Shieh CC, Yen JH, Wang HJ, Su IJ, Lei HY: Antibody to severe acute respiratory syndrome (SARS)-associated coronavirus spike protein domain 2 cross-reacts with lung epithelial cells and causes cytotoxicity. Clin Exp Immunol 2005, 141:500–508
17. Patarca R, Fletcher MA: Structure and pathophysiology of the erythrocyte membrane-associated Paul-Bunnell heterophile antibody determinant in Epstein-Barr virus-associated disease. Crit Rev Oncog 1995, 6:305–326
18. Hayashi K, Ohara N, Teramoto N, Onoda S, Chen HL, Oka T, Kondo E, Yoshino T, Takahashi K, Yates J, Akagi T: An animal model for human EBV-associated hemophagocytic syndrome: herpesvirus papio frequently induces fatal lymphoproliferative disorders with hemophagocytic syndrome in rabbits. Am J Pathol 2001, 158:1533–1542
19. Hayashi K, Teramoto N, Akagi T: Animal in vivo models of EBV-associated lymphoproliferative diseases: special references to rabbit models. Histol Histopathol 2002, 17:1293–1310
20. Hayashi K, Jin Z, Onoda S, Joko H, Teramoto N, Ohara N, Oda W, Tanaka T, Liu YX, Koirala TR, Oka T, Kondo E, Yoshino T, Takahashi K, Akagi T: Rabbit model for human EBV-associated hemophagocytic syndrome (HPS): sequential autopsy analysis and characterization of IL-2-dependent cell lines established from herpesvirus papio-induced fatal rabbit lymphoproliferative diseases with HPS. Am J Pathol 2003, 162:1721–1736
21. Ishii E, Ohga S, Imashuku S, Kimura N, Ueda I, Morimoto A, Yamamoto K, Yasukawa M: Review of hemophagocytic lymphohistiocytosis (HLH) in children with focus on Japanese experiences. Crit Rev Oncol Hematol 2005, 53:209–223
22. Harrington DS, Weisenburger DD, Purtilo DT: Malignant lymphoma in the X-linked lymphoproliferative syndrome. Cancer 1987, 59:1419–1429
23. Yao M, Cheng AL, Su IJ, Lin MT, Uen WC, Tien HF, Wang CH, Chen YC: Clinicopathological spectrum of haemophagocytic syndrome in Epstein-Barr virus-associated peripheral T-cell lymphoma. Br J Haematol 1994, 87:535–543
24. Tabata Y, Villanueva J, Lee SM, Zhang K, Kanegane H, Miyawaki T, Sumegi J, Filipovich AH: Rapid detection of intracellular SH2D1A protein in cytotoxic lymphocytes from patients with X-linked lymphoproliferative disease and their family members. Blood 2005, 105:3066–3071
25. Chuang HC, Lay JD, Hsieh WC, Wang HC, Chang Y, Chuang SE, Su IJ: Epstein-Barr virus LMP1 inhibits the expression of SAP gene and upregulates Th1 cytokines in the pathogenesis of hemophagocytic syndrome. Blood 2005, 106:3090–3096
26. Lay JD, Tsao CJ, Chen JY, Kadin ME, Su IJ: Upregulation of tumor necrosis factor-alpha gene by Epstein-Barr virus and activation of macrophages in Epstein-Barr virus-infected T cells in the pathogenesis of hemophagocytic syndrome. J Clin Invest 1997, 100:1969–1979
27. Lay JD, Chuang SE, Rowe M, Su IJ: Epstein-Barr virus latent membrane protein-1 mediates upregulation of tumor necrosis factor-alpha in EBV-infected T cells: implications for the pathogenesis of hemophagocytic syndrome. J Biomed Sci 2003, 10:146–155
28. Trotta R, Parihar R, Yu J, Becknell B, Allard II J, Wen J, Ding W, Mao H, Tridandapani S, Carson WE, Caligiuri MA: Differential expression of SHIP1 in CD56bright and CD56dim NK cells provides a molecular basis for distinct functional responses to monokine costimulation. Blood 2005, 105:3011–3018
29. Brncić N, Sever-Prebilic M, Crnic-Martinovic M, Prebilic I: Severe autoimmune hemolitic anemia as a potentially fatal complication of EBV infectious mononucleosis. Int J Hematol 2001, 74:352–353
30. Sevilla J, del Carmen Escudero M, Jimenez R, Gonzalez-Vicent M, Manzanares J, Garcia-Novo D, Madero L: Severe systemic autoimmune disease associated with Epstein-Barr virus infection. J Pediatr Hematol Oncol 2004, 26:831–833
31. McClain MT, Heinlen LD, Dennis GJ, Roebuck J, Harley JB, James JA: Early events in lupus humoral autoimmunity suggest initiation through molecular mimicry. Nat Med 2005, 11:85–89
32. Savard M, Belanger C, Tardif M, Gourde P, Flamand L, Gosselin J: Infection of primary human monocytes by Epstein-Barr virus. J Virol 2000, 74:2612–2619
33. Gołaszewska E, Kurowska E, Duk M, Koscielak J: Paul-Bunnell antigen and a possible mechanism of formation of heterophile antibodies in patients with infectious mononucleosis. Acta Biochim Pol 2003, 50:1205–1211
34. Shoenfeld Y: The idiotypic network in autoimmunity: antibodies that bind antibodies that bind antibodies. Nat Med 2004, 10:17–18